



Research article

Quantum chemical investigation of the antiradical property of avenanthramides, oat phenolics



P.C. Sumayya, Godsa Merin Babu, K. Muraleedharan*

Laboratory of Computational Chemistry, Department of Chemistry, Faculty of Science, University of Calicut, Malappuram, 673635, India

ARTICLE INFO

Keywords:

Oats phenolics
Avenanthramides
Density functional theory
Spin density
Donor acceptor map

ABSTRACT

Avenanthramides (AVs) are polyphenolic components found in oats. The present work is devoted to the exploration of structure-based radical scavenging activity of nine AVs; **2p**, **2f**, **2c**, **1p**, **1c**, **1f**, **1s**, **2s**, and **3f**, using M06-2X functional level of density functional theory with basis set 6-31+G(d, p) both in gas and ethanol medium. The act of compounds towards the electron transfer mechanism was analyzed with the help of a Donor-acceptor map (DAM) and classified as antioxidants and anti-reductants. The main mechanism of radical action, HAT, SET-PT, and SPLET were examined and found to be the preference of HAT and SPLET respectively in the gas phase and ethanol medium. The computed quantum mechanical atom in molecule (QTAIM) parameters; the intramolecular H-bonding, Noncovalent interactions, aromaticity also acted as pillars to supports the activity of compounds. The activity was found to be increasing with the stabilizing group ortho to the reactive phenolic OH group.

1. Introduction

Grains are one of the most important dietary components of most of the world's population and are packed with nutrients including proteins, fibers, vitamins, minerals, and antioxidants [1]. A diet rich in the whole grain is associated with a reduced risk of many chronic diseases such as cardiovascular diseases, cancers, and type 2 diabetes [2]. Some of these issues are driven by excess free radicals present in the body [3]. Luckily, an antioxidant-rich diet can help to improve antioxidant levels in the blood and reduce the risk of these diseases. There are too many research papers on both theoretical and experimental research into the antioxidant role of phytochemicals found in fruits and vegetables and are still underway [4, 5, 6]. Nevertheless, cereals are largely ignored as a key contributor to dietary antioxidants.

Avenanthramides (AVs) are secondary metabolites found in oats (*Avena Sativa*, L). These polyphenolic compounds are essential components of oats groats, hull, leaves, and bran and which together contribute 0.2–0.8 mg/g of oats grains [7]. Structurally, AVs are cinnamoyl anthranilic acid derivatives, but as per substitution (hydroxyl group, methoxyl group, hydrogen) on both rings distinguish them from each other [8]. From literature, the major avenanthramides isolated are mainly differed as per substitution on the cinnamic acid part of the avenanthramide molecules [9]. It may be ferulic acid, p-coumaric acid,

caffeic acid, sinapic acid derivatives, and give notations f, p, c, and s respectively in their simplest representations. Avenanthramides according to substitution on the anthranilic acid part are reported, but little in number [10]. These low molecular weight, soluble polyphenol compounds have been shown to possess beneficial biological properties including anti-inflammatory, antiatherogenic, antiproliferative, anti-cancer, anti-itch that may be useful in the prevention of coronary heart diseases and cancers [11]. Different commercial oat products are available on the consumer market as rich sources of phenolic acids and avenanthramides [12, 13].

The compounds such as α -tocopherol, various hydroxyl cinnamate esters of long-chain alcohols, hydroxy fatty acids, Vallin, caffeic acids, etc., are also included as antioxidant compounds in oats in the company of AVs [10, 14, 15]. Such compounds protect lipids from oxidation and enable long-term stabilization of the grains of oats. The derivatives of α -tocopherol and cinnamic acid are highly sensitive to oxygen use, and also heat and light. The long-lasting antioxidant function of oat grains can, therefore, be expected to come from the polyphenolic components AVs [10]. Hence the storage and heat stability of oats grains are concerned polyphenol AVs can persist its activity for a long time than polyphenol present in the fruits and vegetables. Therefore more attention needs to be paid to grains that contain antioxidant AV compounds.

* Corresponding author.

E-mail address: kmuralika@gmail.com (K. Muraleedharan).

The antioxidant activities of oat grains are first suggested independently by Lowen et al (1937), and Peters and Musher (1937) [1]. About 50 years later, Collin identified around 40 Avenanthramides (hydroxy or methoxy) derivatives that are responsible for the antioxidant activity of oat grains [8] and the complete structural analyses of the 10 AVs are successfully identified spectrometrically [8]. Literature mainly focused on avenanthramides, **2p**, **2c**, and **2f** in discussions of antioxidant activity of oats phenolics. In vitro, antioxidant studies using different assays; NORAC, SORAC, ORAC, SOAC, and HORAC respectively for peroxynitrite, superoxide anion, peroxy radicals, singlet oxygen, and hydroxyl radicals reported that activity **2c** was 1.5 fold than **2p** and **2f** [10–12,16, 17].

While there have been several experimental studies on the chemical and biological properties of avenanthramides, only a handful of them has been computationally examined [10]. Uses of computational chemistry tools in research are a "must-have" tool for the scientific community. This multidisciplinary field of research provides fundamental properties of atoms and molecules using quantum mechanics and thermodynamics. In this situation, systematic investigations on the structural and free radical scavenging tendencies of AVs and their capacity to scavenge free radicals are needed. The radical scavenging action between oats molecule and free radical can be of anti-oxidation (antioxidant) or anti-reduction (anti-reductant) of AV molecules. Considering the abundance of **2p**, **2c**, and **2f**, works of literature mainly reported antioxidant activity of these avenanthramides, and others are ignored.

This work aimed to study the antiradical potency of avenanthramide found in oats. So the radical scavenging action against a free radical can be either by transfer of an electron between them or by transfer of hydrogen atom or by proton transfer or maybe both. In the situation of absence of computational works in this area, and the absence of more kinds of literature on the detailed study, as like electron transfer deactivation or hydrogen atom transfer deactivation of free radicals, more spaces of research are found in this field along with a discussion on antioxidant or anti-reductant tendencies.

The present work studies the structural and antiradical characteristics of the compounds, N-(4'-hydroxy-(E)-cinnamoyl)-5-hydroxyanthranilic acid (**2p**), N-(4'-hydroxy-3'-methoxy-(E)-cinnamoyl)-5-hydroxyanthranilic acid (**2f**), N-(3', 4'-dihydroxy-(E)-cinnamoyl)-5-hydroxyanthranilic acid (**2c**), N-(4'-hydroxy-(E)-cinnamoyl)-anthranilic acid (**1p**), N-(3', 4'-dihydroxy-(E)-cinnamoyl)-anthranilic acid (**1c**), N-(4'-hydroxy-3'-methoxy-(E)-cinnamoyl)-anthranilic acid (**1f**), N-(4'-hydroxy-3',5'-dimethoxy-(E)-cinnamoyl)-anthranilic acid (**1s**), N-(4'-hydroxy-3',5'-dimethoxy-(E)-cinnamoyl)-5-hydroxyanthranilic acid (**2s**), N-(4'-hydroxy-3'-methoxy-(E)-cinnamoyl)-5-hydroxy-4-methoxy anthranilic acid (**3f**) employed using computational methodologies.

2. Materials and method

2.1. Computational method

All calculations described in this work were performed with the Gaussian 09W computational programming package [18]. The molecular structures of AVs are downloaded from the PubChem database [19] in SDF file format and converted GJF file using OpenBabel application [20]. Density functional theory (DFT) has been adopted for calculation among various computational calculation tools because it is a convenient method for predicting the physical and chemical properties with great accuracy. Besides, DFT allows the determination of all properties by electron density as a function of three variables (X, Y, Z) and therefore suitable for free radical scavenging action, since both are based on electron density. According to the literature, from the family of Minnesota Functionals, M05-2X [21] and M06-2X [22] functional seem to give good results for the free radical reactions. Hence, considering top performance within the 06 functionals for main group thermochemistry, kinetics, and non-covalent interactions over B3LYP functional, the M06-2X suite of DFT are selected for the study with 6–31 + G (d, p) basis

set. The comparison of experimental ¹HNMR of **2p** with theoretical ¹HNMR using different levels of theories is given in Table S1 [8]. The solvent effect was described by the IEFPCM solvent model in the ethanol environment, because, it is one of the soluble media for AVs [1]. The vibrational frequencies were performed at the same level to confirm all of the stationary points as minima (zero imaginary frequency). The geometry optimization of neutral molecules, its radicals, cations, and anions are optimized in the same level of theory to obtain the descriptors like BDE (Bond Dissociation Enthalpy), IP (Ionization Potential), PDE (Proton Dissociation Enthalpy), PA (Proton affinity), and ETE (Electron Transfer Enthalpy) needed for radical scavenging activity in the ground state in the gas phase and ethanol media. Moreover, the weak noncovalent interactions and spin density computations of AVs have been carried out using Multifunctional Wave function Analyzer, Multiwfn 3.3.8 suite [23] using M06-2X/6–31 + G (d, p) level of theory.

2.2. Atom in molecule (AIM) analysis

The "Quantum Theory of Atoms in Molecules (QTAIM)" proposed by Bader [24] discloses the covalent and non-covalent interactions between atoms in light of electron density $\rho(r)$ and its Laplacian $\nabla^2\rho(r)$ at the bond critical points (BCP), a region between a pair of nuclei where $\nabla\rho(r) = 0$. From the BCP parameters obtained from the QTAIM study, such as the Lagrangian kinetic electron density (g) and the potential electron density (v), total energy density (H), the existence of stabilizing interactions between nuclei can be studied, which are quite significant in dealing with the radical scavenging behavior of substances. The nature of stabilizing interaction, type of bond, bond strength, and energy of hydrogen bond (E_{HB} ; Equation 1) [25] between nuclei of interest can also be examined. Since the entire work concerns the antiradical properties of polyphenol, avenanthramides obtained from oats, BCP parameter evaluation is critical. The Poincaré-Hopf relationship of all critical points is evaluated and found to be valid in all topological analysis of AVs instances. QTAIM was performed using a multiwfn 3.3.8 suite.

$$E_{HB} = 1/2(V_{BCP}) \quad (1)$$

2.3. Non-covalent interaction (NCI) analysis

Using quantum-mechanical electron density and its derivatives, qualitative and quantitative analyzes of non-covalent molecular interactions in real space can be explored using the approach reduced gradient density (RDG) [26]. It is a fundamental dimensionless quantity used in DFT to define the deviation from the homogeneous distribution of electrons and gives a rich description of van der Waals interactions, hydrogen bonds, and steric repulsions in molecules. The definition of the RDG function is shown in Eq. (2) below (see Figure 1).

$$RDG(r) = \frac{1}{2(3\pi^2)^{1/3}} \frac{|\nabla\rho(r)|}{\rho(r)^{5/3}} \quad (2)$$

To visualize the obtained isosurfaces of NCI analysis, the visual molecular dynamics (VMD) molecular graphics program was used. Plots of reduced density gradient (RDG) versus the electron density multiplied by the sign of the second Hessian Eigenvalue, as in Figure 2.b, reveals the basic pattern of intramolecular interactions. In three dimensional spaces, the weak interactions are the reduced density gradient (RDG) at low densities appears as colored regions (isosurfaces). These regions are defined as strong attractive interactions, weak interactions, and strong repulsive interactions.

2.4. Donor acceptor map (DAM)

The relative feasibility to donate, or accept, charge or electron from set chemical compounds to another can be represented with the help of

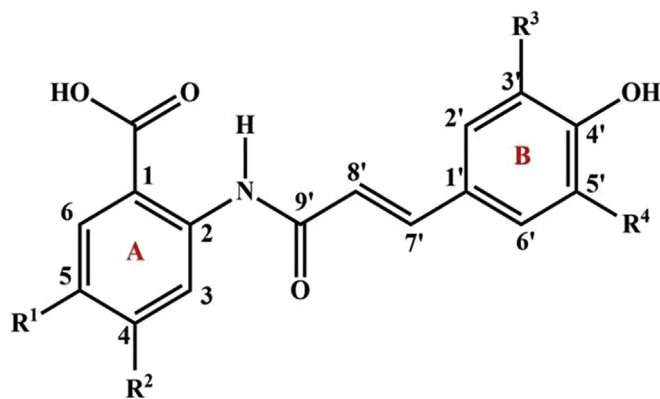


Figure 1. Chemical structures of the oats avenanthramides (p = p-coumaric acid, f = ferulic acid, c = caffeic acid and s = sinapic acid).

donor-acceptor map (DAM). The molecule's tendency to act antioxidant and anti-reductant towards the free radicals can easily be analyzed. The schematic diagrams of the donor-acceptor map are given in Figure 4. The Ra and Rd are respectively the electron acceptance and electron donation indexes [27] calculated from ionization energy (IE) and electron affinity (EA) of the molecules as follows,

$$Ra = \frac{\omega_L^+}{\omega_F^+} \quad (3)$$

$$Rd = \frac{\omega_L^-}{\omega_{Na}^-} \quad (4)$$

ω^- & ω^+ are the tendencies of a compound to donate and accept electron respectively and these parameters can be computed using the method (5) & (6) [28]. The electron-accepting and electron-donating power of a molecule L are represented for F and Na respectively.

When $\omega_L^+ \cong \omega_F^+$; L and F are equally efficient electron acceptors.

$\omega_L^+ \gg \omega_F^+$; L is more efficient than F.

$\omega_L^- \cong \omega_{Na}^-$; L and F are equally efficient electron donors.

$\omega_L^- \ll \omega_{Na}^-$; L is more efficient than Na

$$\omega^- = \frac{(3IE + EA)^2}{16(IE - EA)} \quad (5)$$

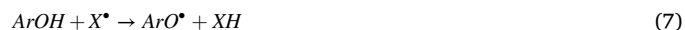
$$\omega^+ = \frac{(IE + 3EA)^2}{16(IE - EA)} \quad (6)$$

2.5. Free radical scavenging activity

Radical scavenging activity of phenolic antioxidants theoretically expressed mainly by three possible mechanisms, namely, Hydrogen atom transfer (HAT) mechanism, Single-electron transfer followed by proton transfer (SET-PT) mechanism and Sequential proton loss electron transfer (SPLET) mechanism [29, 30, 31, 32, 33, 34] and were calculated under standard conditions of 1 atm. and 298.15 K.

1. HAT (Hydrogen atom transfer) mechanism

The antioxidant (ArOH) scavenges the free radical (X^\bullet) by the transfer of the hydrogen atom of -OH group to the radical species, and become phenoxide radical. The corresponding controlling parameter associated with the HAT mechanism is bond dissociation enthalpy (BDE). Lower BDE indicates good antioxidant activity. If the antioxidant contains more than one -OH group, then the homolytic cleavage occurs to all the -OH present depending on the BDE of the -OH. The one with lower BDE, easier will be the cleavage of O-H bond and contribute more towards the antioxidant activity.



2. a) SET (Single electron transfer) mechanism

In this mechanism, the reactive free radicals are neutralized by making them anions through the transfer of electrons to it. These electrons are provided by the most reactive hydroxyl groups from polyphenolic compounds. The antioxidant compound then becomes a radical cation. The corresponding controlling parameter associated with this mechanism is AIP (adiabatic ionization potential). The mechanism involved is



b) SET-PT (Single electron transfer followed by proton transfer) mechanism

This is a two-step mechanism, in which the first step is an electron transfer from the antioxidant and the second step is a proton transfer from the radical cation formed in the first step.



In SET-PT mechanism first step is by ionization potential (IP) or electron transfer capacity and the second step is heterolytic O-H bond cleavage. The corresponding controlling parameter associated with the second step is proton dissociation enthalpy (PDE).

3. SPLET (Sequential proton loss electron transfer) mechanism

This is also a two-step mechanism, in which the first step is the dissociation of the antioxidant into phenoxide anion and proton. Then the phenoxide anion formed in the first step reacts with free radicals at specific pH; products formed are similar to those obtained in the HAT mechanism. The corresponding controlling parameter associated with the first step is proton affinity (PA) and the second step is electron transfer enthalpy (ETE).



3. Results and discussion

3.1. Optimized structures of avenanthramides

To elucidate the relationship between the molecular structure and the radical scavenging activity, the analysis of the conformation and geometric characteristics of the compounds considered are significant. Due to the $O=C-C\alpha=C\beta$ bond, this class of molecules will exist in different isomers for the A ring and the B ring. Concerning $C=C$, the molecule may exist cis or trans isomer, because of the steric clash from the B ring, thermodynamically trans one is more stable than cis. In this trans isomer, there may be two conformations due to $O=C-C\alpha=C\beta$ bond, s-trans and s-cis. The previous experimental studies reveal the stability of s-cis than s-trans. This kind of conformational quest is carried out as inspired by the chalcone conformation analysis [35]. Therefore all molecules are called the trans-s-cis conformer throughout the analysis.

The potential energy scan of molecules was carried out by varying the dihedral angle values in 12 steps of 30° from 0 to 360° at the B3LYP/6-21G level of theory. Potential energy profile plots are shown in Fig. S1-S11. The 3D potential energy surface and the structure correspond to the global minimum of **2p** are shown in Fig. S1. The PES diagram containing

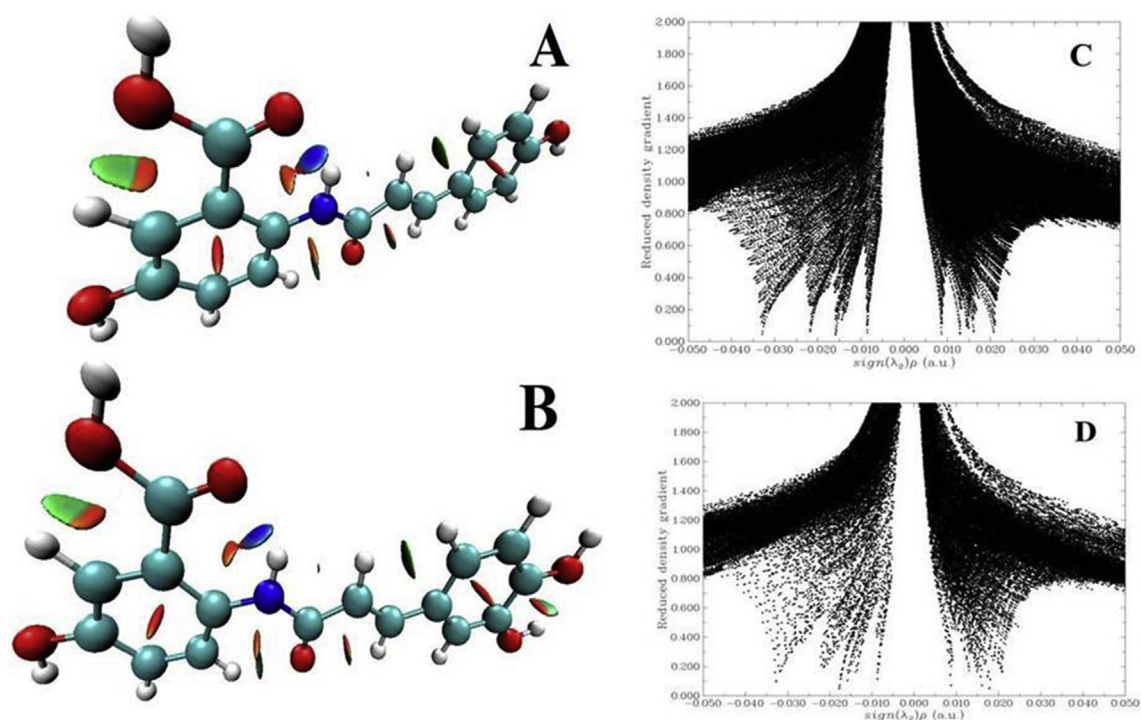


Figure 2. A & B are color-filled RDG map showing non-covalent interactions of 2p and 2c respectively. The hydrogen bonds are displayed in blue, van der Waals is presented in light green and steric repulsions are shown in red. C & D are the plots of the reduced density gradient versus the electron density multiplied by the sign of the second hessian eigenvalue, $\text{sign}(\lambda_2)\rho$ of 2p and 2c respectively.

dark blue, light blue, and dark red, light red colored grids represents global minimum, local minimum, local maximum, and global maximum respectively. The better conformers with the lowest energy of all structures are considered and these structures are further considered for energy minimization.

After minimum energy conformation was obtained, further geometry optimization was performed with M062X/6-31+G(d,p) level of theory. The geometry optimized structures of all AVs are presented in Fig.S12. Vibrational frequency calculations were performed at the same level to confirm the absence of imaginary frequencies. The bond length and bond angles of 2p, 2f, and 2c are provided in Table S2 and S3 respectively. The optimized XYZ coordinates of 2p in the gas phase are also provided in Table S4. An intramolecular hydrogen bonding (IHB) between the carbonyl oxygen of carboxylic acid and the NH group was seen in all optimized AV structures. Therefore, it is predicted that these IHB would prefer coplanarity between the A-ring, bridging chain, and the B ring. From the data of dihedral angles Table S5 of AV neutral molecules at Φ (C4, C3, C2, N) and Φ (C3', C2', C1', C7'), it can be observed that the compounds 2p, 2c, 1p, 1c, and 1f are completely planar and 2f, 1s, 3f, and 2s are very slightly deviating from planarity.

The radicals (ArO), cations (ArO⁺) radicals, anions (ArO⁻) have also been optimized using the same method, starting with the optimized structure of neutral AV molecules by removing hydrogen atoms from successive positions. By comparison, no major geometrical shift was observed when moving from neutral to the corresponding radical, cation radical, and anionic forms except for NH. When radical/anion is formed from NH group of molecules some degree of distortion from planarity to the ring A has been observed due to disappearance of IHB between NH and C=O group and other part ring B has found to keeping its planarity with the O=C- α =C β bond. In Table S6, the dihedral angles Φ (C4, C3, C2, N) and (C3', C2', C1', C7') of anion and radical of each reactive sites are given and supports the above observation.

The properties of a compound can be derived from its ground-state electron density $\rho(r)$ and the essence of a molecule's structure can be obtained within the topology of $\rho(r)$. A chemical reaction is preceded

by $\rho(r)$ redistributions, and the methods that analyze $\rho(r)$ distributions should help to understand the electron structure of molecules and thus chemical reactivity. Spatial topological decomposition of $\rho(r)$ itself is the basis of the popular Atoms in Molecules (AIM) theory, which will be a mathematical tool to describe the properties of chemical systems and to extract observable information from the electron density. As an extension of the AIM theory, Johnson and co-workers introduced the concept of Non-Covalent Interactions (NCI) index [26], which has been specifically developed to reveal non-covalent interactions, such as hydrogen bonding, Van der Waals, steric interactions in three-dimensional spaces.

Table 1 clearly explains quantitatively the nature of hydrogen bonding interaction between the stabilizing groups, which are very essential for dealing with the antiradical properties of polyphenols, using the parameters of QTAIM theory. The parameters, electron density ($\rho(r)$), its second derivative or Laplacian of electron density ($\Delta^2\rho(r)$), lagrangian kinetic electron density ($g(r)$), potential electron density ($v(r)$), total energy density ($g(r) + v(r)$), hydrogen bond energy (E_{HB}), at BCP, were analyzed.

From Table 1, the nature hydrogen bonding can be examined as follows, 1) for strong hydrogen bond, the parameters should be $\nabla^2\rho(r) < 0$, and $g(r)+v(r) > 0$, 2) for intermediate type of hydrogen bond, it should be $\nabla^2\rho(r) > 0$, and $g(r)+v(r) < 0$, and for weak hydrogen bonds, $\nabla^2\rho(r) > 0$, and $g(r)+v(r) > 0$. For NH—CO interaction, the values $\nabla^2\rho(r)$ and $g(r) + v(r)$ are greater than zero except for 3f indicating the existence of weak hydrogen bonding interaction. However, in case of 3f, the positive value of $\nabla^2\rho(r) (>0)$ and negative values of $g(r)+v(r) (<0)$ designates the intermediate hydrogen bonding interaction may be due to activating functional group OCH3 para to the COOH.

The nature hydrogen bonding interaction between OH... OCH3 of compounds 2f, 1f, 1s, 2s, and 3f are also represented in Table 1. The positive values of $\nabla^2\rho(r) (>0)$, and $g(r) + v(r) (>0)$ reveals very weak hydrogen bonding interaction between OH... OCH3.

Moreover, the negative value of E_{HB} for NH—CO and OH—OCH3 of all compounds indicates that these interactions are thermodynamically

feasible. Since the magnitude of the E_{HB} is about the strength of the hydrogen bond, the NH ... CO interactions are relatively stronger than the OH ... OCH₃ interactions. For the compounds, **1s** and **2s**, both the ortho positions of OH having an OCH₃ group (HOC⁴-C⁵OCH₃ and HOC⁴-C³OCH₃) and these OH can either form hydrogen bonding interaction with C⁵OCH₃ or C³OCH₃. The magnitude of E_{HB} significantly reveals the hydrogen bonding strength of OH with C⁵OCH₃ over C³OCH₃ interaction. This observation supports the conformational study of these compounds which are explained pictorially in supporting information (Fig. S8-Fig. S10). For the compound **3f** having another OH... OCH₃ interaction on A ring (HOC⁵-C⁴OCH₃) in addition to (HOC⁴-C⁵OCH₃) of B ring. The strength of hydrogen bond bonds is found to be almost similar.

The NCI isosurfaces of **2p** are represented in Figure 2.a. and the remaining compounds in Fig.S13. Based on the second derivative of the hessian matrix a continuous color-coding scheme is used. The surfaces are displayed on a blue-green-red scale concerning the values of sign (λ_2) ρ , ranging from -0.05 to 0.05 a.u. The strong attractive interactions related to hydrogen bonds are represented in blue, weak interactions like van der Waals in green, and strong repulsive interactions in red. Visual inspection of AVs clearly illustrates the hydrogen bonding interaction between the C=O of carboxylic acid and the NH group in all compounds with the blue colored region. The NCI isosurfaces shown between the C=O of carboxylic acid and NH (like a dumbbell shape) is a mixture of blue and orange color represents the presence of critical points where distinct blue region centered at the BCP corresponding to a moderate hydrogen bonding interaction and a distinct yellow region centered at the ring critical point. For the compound **3f**, the NCI isosurfaces (Fig.S13) between the C=O of carboxylic acid and the NH group are clearly shown as small spheres corresponding to BCP (blue) and RCP (orange) critical points.

For compounds **2c** and **1c** apart from the C=O and NH hydrogen bonding interaction, one more such interaction is there in the compound due to catechol moiety on the B-ring. Using the BCP criteria of AIM theory this interaction couldn't be proved due to the absence of BCP between the catechol moieties. The NCI isosurfaces obtained between these two hydroxyl groups is a small sphere of color red-green represents the collapse of two critical points BCP and RCP (ring critical point; a second-order saddle point found at the center of the ring). Hence it is difficult to find the nature of interaction in that region due to the absence of BCP using this theory. But it doesn't mean the absence of hydrogen bonding, but only as of the absence of a single piece of evidence of hydrogen bonding using this theory [36].

The plot of reduced density gradient (RDG) versus the electron density multiplied by the sign of the second Hessian Eigenvalue (refer Figure 2b)) can explain noncovalent interactions clearly. One or more spikes in the low density, the low gradient of the plot are significantly distinguishing noncovalent interactions. If it is a hydrogen bonding interaction, these lies in the negative value region, for the sterically crowded region remains at positive values indicating the lack of bonding that area of the molecule, and spike at very near zero denotes the van der Waals interaction. The RDG Vs sign (λ_2) ρ curves of **2c** given in Figure 2 are not qualitatively different than other AVs given in Fig.S14. In all cases, the trough at negative sign (λ_2) ρ corresponds to hydrogen bonding interactions.

The aromaticity of each benzene ring was calculated using three methods to identify the reactivity of the molecules. The three methods; harmonic aromatic oscillator model (HOMA) [37], aromatic fluctuation index (FLU) [38], and para-delocalization index (PDI) [37] are used and the result was compared. If the HOMA value equal to 1, then the ring is fully aromatic. The higher the value of PDI, the delocalization will be larger, and the stronger the aromaticity. Lower FLU corresponds to stronger aromaticity. The aromatic indices of ring A and B correspond to each AVs are given in Table S7. Analyzing all these aromatic indexes, it is found that ring B is more aromatic than ring A.

3.2. Donor acceptor map (DAM)

According to the direction of charge transfer, the compound can act as either an antioxidant (donor of an electron) or anti-reductant (acceptor of an electron). The donor accepting tendencies of compounds can be studied with the help of IE and EA values. However, when describing the charge transfer of antiradical, it is better to state in terms of its electron-donating (ω^+), and electro-accepting (ω^-) capacity as shown in equation 5 & 6, than IE and EA values. The low value of ω^- indicates a stronger tendency to donate an electron, while, a high value of ω^+ suggests the greater propensity to accept an electron. The increasing order of ω^- in gas phase is **3f** < **2f** < **2s** = **2c** = **2p** < **1f** = **1s** < **1p** < **1c** and in ethanol is **2p** < **3f** < **2f** < **2c** < **2s** < **1s** < **1p** = **1c** < **1f**. The increasing order of ω^+ in gas phase is **3f** < **2f** < **2p** = **2c** = **2s** = **1f** < **1s** = **1p** = **1c** and **2p** < **2f** = **2c** < **1p** < **3f** < **1c** = **2s** < **1f** = **1s** (Table S9 & S10).

DAM plot simultaneously shows the electroacceptance and the electrodonating power of the compounds concerning good electron acceptor atom F (as Ra index) and good electron donor atom Na (as Rd index).

The plot containing four quadrants (separating lines are symbolic to help imagine), a worst antiradical region, where bad electron acceptors and bad electron donors (Ra small and Rd large); a best antiradical region, where the compounds are good acceptors and good donors (Ra large and Rd small); a good anti-reductant region, where compounds are good electron acceptors (Ra and Rd large); and good antioxidant region, where compound acts as good donors (Ra and Rd small). Since anti-reductant and antioxidant compounds are also good antiradical, three of the four regions are for good antiradical compounds.

The DAM plots of compounds examined are shown for the gas phase and ethanol in Figure 3. Ionization potential, electron affinity, ω^- , ω^+ , Ra, and Rd in the gas phase and ethanol are tabulated in Table S9 & S10. It is shown that Rd >1 and Ra <1, poor electron donating and electron accepting power of AVs compared with Na and F respectively, both in the gas phase and ethanol. In the gas phase, **2c**, **2s**, **1f**, and **1s** are the best antiradical with good electron-accepting and donating tendencies. The compounds, **2p**, **2f**, and **3f** tend to donate electrons during radical scavenging action and hence in the gas phase are the good antioxidants. Similarly the compounds **1p** and **1c** can accept electron charge and acts as good anti-reductant in the radical deactivation process.

From Figure 3, it is clear that, in ethanol, the avenanthramide **1p** exhibits the worst antiradical property, indicates that they are not suitable to donate or accept electrons in comparison with others. In this solvent, remaining AVs situate only in two quadrants, where, **1c**, **1f**, **1s**, and **2s** as good anti-reductants, and **2p**, **2f**, and **2c** as good antioxidants. When the solvent changes from the gas phase to ethanol, the electron transfer tendencies of the compounds also changes. Apart from analyzing the antiradical property by the movement of electrons, the other tendencies of deactivating free radical species are by transfer of hydrogen atom from its phenolic OH or NH groups of compounds and are explained in continuing sections.

3.3. Radical scavenging mechanism study

Three radical scavenging mechanisms are discussed, HAT, SET, and SPLET. The HAT mechanism is completely a hydrogen atom transfer mechanism, whereas the SET and SPLET mechanism involves both electron transfer and proton transfer. Various antioxidant descriptors corresponding to the mechanism of free radical scavenging action were calculated in the gas phase and ethanol solution are presented below.

3.3.1. Analysis of HAT mechanism

The calculated BDE values of AVs in both the gas phase and solvent ethanol are shown in Table S8. The energy of bond dissociation is the best parameter to explain a molecule's radical scavenging activity because hydrogen bond strength dictates the efficacy of hydrogen abstraction.

Table 1. BCP parameters of intermolecular hydrogen bonds: electron density, Laplacian of the electron density, and hydrogen bond strength (kcal/mol) (calculated from M062X/6-31+G(d,p) wave function in the gas phase) for Avenanthramides.

	BCP parameters					
	$\rho(r)$	$g(r)$	$v(r)$	$g(r)+v(r)$	$\Delta^2\rho(r)$	E_{HB} (kcal/mol)
NH—CO						
2p	0.03290	0.02840	-0.02830	0.00002	0.11353	-8.87926
2f	0.03310	0.02850	-0.02840	0.00001	0.11394	-8.91064
2c	0.03289	0.02829	-0.02827	0.00002	0.11328	-8.86985
1p	0.03363	0.02890	-0.02888	0.00002	0.11564	-9.06124
1c	0.03378	0.02903	-0.02901	0.00002	0.11618	-9.10203
1f	0.03388	0.02911	-0.02909	0.00002	0.11653	-9.12399
1s	0.03361	0.02887	-0.02885	0.00002	0.11556	-9.05183
2s	0.03267	0.02811	-0.02809	0.00002	0.11257	-8.81337
3f	0.0335	0.02744	-0.02876	-0.00132	0.11492	-9.03614
OH... OCH3						
2f	0.01976	0.02014	-0.01838	0.00176	0.08760	-5.76681
1f	0.01973	0.02013	-0.01836	0.00177	0.08759	-5.76054
1s (HOC4'-C5'OCH3)	0.02014	0.02047	-0.01876	0.00171	0.08873	-5.89859
1s (HOC4'-C3'OCH3)	0.01311	0.01123	-0.01010	0.00113	0.04941	-3.16892
2s (HOC4'-C5'OCH3)	0.02011	0.02045	-0.01873	0.00172	0.08865	-5.87977
2s (HOC4'-C3'OCH3)	0.01289	0.01105	-0.00914	0.00191	0.04873	-2.86772
3f (HOC5-C4OCH3)	0.01932	0.01985	-0.01798	0.00187	0.08689	-5.64131
3f (HOC4'-C5'OCH3)	0.01975	0.02014	-0.01837	0.00177	0.08762	-5.76368

Here, the free radicals are deactivated by the transfer of a hydrogen atom from the molecule. In a compound with more than one phenolic hydroxyl group, the lowest energy compound is called for a radical scavenging mechanism. The optimized structure of radical species and their spin density distributions for each of the AV after radical formation are analyzed (Figure 4 & Fig.S15–S22). The BDE values both in the gas phase and ethanol are represented in Table S8. The highest BDE for carboxylic-OH functionality (greater than 110) in the gas phase is found in all studied cases of AV, so this is the least reactive site for radical formation reaction. As discussed above, the phenolic NH groups in all AV forms intramolecular interaction (IHB) with the adjacent carbonyl oxygen of carboxylic functionality. Hence the abstraction of the H atom from this N–H implies the breaking of IHB. This will cause a higher BDE of the N–H group. The BDE value of NH in all cases is around 104–108 kcal/mol. Since the BDE values of COOH and NH are above 100 kcal/mol and hence, H atom donation reactions may be overlooked for these two functional groups.

The spin density distribution (SD) [39] and delocalization index (DI) [40] given in Table 2 and the SD distribution isosurface diagram in Figure 4 also supports these observations. When the H abstraction takes place from COOH functional group and forming COO radical, the formed electron density at O radical delocalizes only at the functional group itself not to the ring, hence lower the stability of these radicals. These observations are depicted in Figure 4. The greater SD value of 0.153 indicates that the electron density concentrate on that region itself. DI values of a radical quantitatively explain the extent of the delocalization of that radical [40, 41]. The lower the SD, the higher the DI implies that the one-electron formed at a site are more delocalized and hence stable. Hence, the DI of COO radical is quite higher not means it as a contradictory result, but it is due to continuous delocalization within COO radical. The higher SD and lower DI values of nitrogen radical when compared to other radical, except COO radical also supports the lower stability of radical formed. Hence due to two reasons; the IHB and the low delocalization of radical formed, the involvement of these two functional groups can be neglected from radical scavenging activity.

For the compound **2p**, among the two phenolic hydroxyl groups the lowest BDE value is obtained for 5 OH (84.81 kcal/mol) than the 4' OH (108.11 kcal/mol), hence the activity of **2p** is through 5 OH. The SD and

DI values also suggest the stability of radicals formed from the 5 OH. In ethanol, the same trend in BDE is obtained for 5 OH (85.10 kcal/mol) and 4' OH (87.07 kcal/mol). But the change is lowest for 4' OH may be due to the stabilization of the radical formed by the solvent.

The molecule **2f** also contains two hydroxyl groups on both A and B rings and 5 OH (84.75 kcal/mol) of the A ring exhibits lower energy for bond dissociation than the 4' OH (86.23 kcal/mol) of the B ring. However, a methoxy group in the ortho of donor hydroxy group, considerable enhancement in activity is observed. In **2c**, when ortho of a donor hydroxyl group, 4' OH substituted with another hydroxyl group resulted in an enhanced activity than methoxy substituted molecule with BDE of 77.87 kcal/mol. The other hydroxyl groups present in the B ring and A ring respectively are 89.19 kcal/mol (3'OH) and 84.87 kcal/mol (5 OH). From these two avenanthramides, more than one conclusion can be made according to their bond dissociation energy values. Firstly, the hydroxyl group present on the B- ring is more active than the A-ring, secondly, 4' OH will be the donor hydroxyl group due to extended delocalization of radicals formed through the molecule and is supported by SD and DI values given in Table 2, and thirdly hydroxyl group in the ortho position of donor hydroxyl group can enhance the activity by stabilizing the radical formed more than the methoxy group, and finally, the substitution on B-ring doesn't affect on the hydroxyl group of A ring. All these computationally obtained observations are correlating well with previous experimental conclusions made by authors in this field [9, 10].

The BDE values of donor hydroxyl group (4' OH) of **1p**, **1c**, **1f**, **1s** and **2s** respectively are 86.51 kcal/mol, 78.02 kcal/mol, 86.34 kcal/mol, 82.29 kcal/mol and 82.27 kcal/mol. Comparing **1c**, **1s**, and **2s**, stabilization of radical formed in donor hydroxy group happens more in the presence of hydroxyl group at the nearest position than a dimethoxy group. But, **2f** changed to **1s** and **2s**, enhanced activity was observed due to two methoxy groups on either side of the radical formed. The two hydroxyl groups of **3f** are found to be equally contributing towards radical scavenging activity through their 5 OH with BDE of 86.08 kcal/mol and 86.23 kcal/mol of 4'OH. The SD and DI values tabulated in Table 2 and the isosurface plots (Fig.S15, 16, 17, 18, 19, 20, 21, and 22) are also supporting this HAT mechanism in all studied samples. According to HAT mechanism, the order of radical scavenging activity among the AVs are in the order of **2c** > **1c** > **2s** > **1s** > **2f** > **2p** > **3f** > **1f**

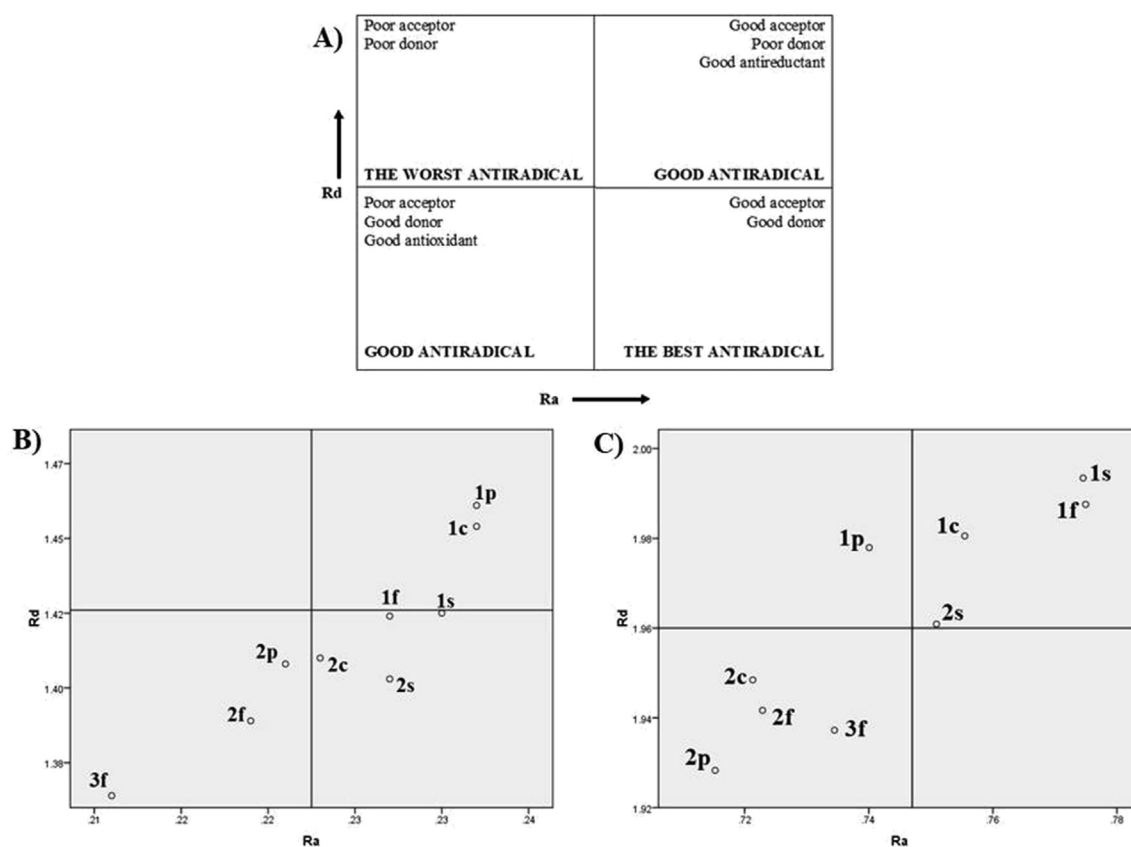


Figure 3. DAM plots of AVs A) model, B) in the gas phase, and C) in ethanol.

> **1p** exactly follows the order caffeic acid > sinapic acid > ferulic acid > p-coumaric acid suggested by the experimental observations [9, 10].

3.3.2. Analysis of SET-PT mechanism

In this mechanism, the radical scavenging molecule ArOH upon electron donation in presence of free radical species results in the formation of a radical cation $\text{ArOH}^{\bullet+}$ and further subsequent deprotonation from the first intermediate forms the corresponding radical ArO^{\bullet} . In this two-step mechanism, the associated numerical descriptors respectively are the IP (ionization potential) and PDE (proton dissociation enthalpy). These global and local reactivity descriptors can have to tell something about the radical scavenging activity of the molecule. Low IP molecules are more vulnerable to ionization and have strong antioxidant properties.

The calculated IP and PDEs of all compounds in both gas phase and ethanol are summarized in Table S8. From Table, it can be found that the lowest IP is found for **3f** irrespective of media implies that electron donation ability is higher for this molecule. The increasing order of electron donation in terms of IP in gas phase is $3f < 2s < 2f < 2p < 1s < 2c < 1f < 1c < 1p$. The order is exactly different when the solvent changes to ethanol, the increasing order of IP is $3f < 1f < 2p < 2f < 2s < 1s < 1c < 1p < 2c$. When turning solvent from gas to ethanol the shift in IP is 46 kcal/mol. These patterns differ greatly from BDE because the IP value is influenced by the whole molecule structure while the BDE is affected by the local phenomena induced by the substituent.

3.3.3. Analysis of SPLET mechanism

In the SPLET mechanism, loss of proton followed by electron transfer from AV is considered. The descriptors associated with the first and second stages of these reactions are represented by PA and ETE respectively. The bond with the highest acidity is involved in PA. Lower the PA, then higher the reactivity. The differences in the PA

values between gas and ethanol are approximately 250 kcal/mol. The gas-phase PA values are in the range of 350 kcal/mol but in ethanol less than 60 kcal/mol. Hence the PA mechanism rises only in polar solvents.

By comparison, we can see that the PA of NH is always higher than all other bonds, shows the reluctance of this group to form anion by releasing a proton from it. It may be due to the strong IHB interaction with the carbonyl of the carboxylic group. In ethanol, the PA values are shown to be the lowest for the carboxylic hydroxyl group due to the stabilization anion formed from the solvent. This is a purely obvious observation because these molecules exist in a solvent cage of ethanol and the proton of the acid group is ready to go to solvent because of the electromeric effect of carbonyl carbon. The anion formed will delocalize continuously through the acid group itself. The increasing order of PA for carboxylic proton donation are $2s < 2f < 1s < 1p < 1f < 2p < 2c < 1c < 3f$. The increasing order of PA of phenolic protons 4' OH of **1c** (41.51 kcal/mol) < 4' OH of **2c** (41.52 kcal/mol) < 4' OH of **1p** (45.57 kcal/mol) < 4' OH of **2p** (45.91 kcal/mol) < 4' OH **1s** (46.64 kcal/mol) < 5 OH of **2s** (46.66 kcal/mol) < 4' OH of **1f** (47.93 kcal/mol) < 4' OH of **3f** (47.98 kcal/mol) < 4' OH of **2f** (48.32 kcal/mol).

In conclusion, as discussed above the preferred descriptors corresponding to HAT, SET-PT, and SPLET are BDE, IP, and PA respectively. These descriptors are therefore used to determine the thermodynamically preferred mechanism for the radical scavenging activity of the compounds studied. Because of the lowest value of BDE relative to other descriptors, it could be found from the above discussions that HAT would be the optimal pathway for these molecules in the gas phase or vacuum. So in the gas phase free radicals deactivate by the transfer of hydrogen atom from the compound. But the medium turning to ethanol, the PA pathway overtakes the HAT and SET-PT mechanisms. SPLET would, therefore, be the preferred mechanism to explain radical scavenging activity in the polar medium.

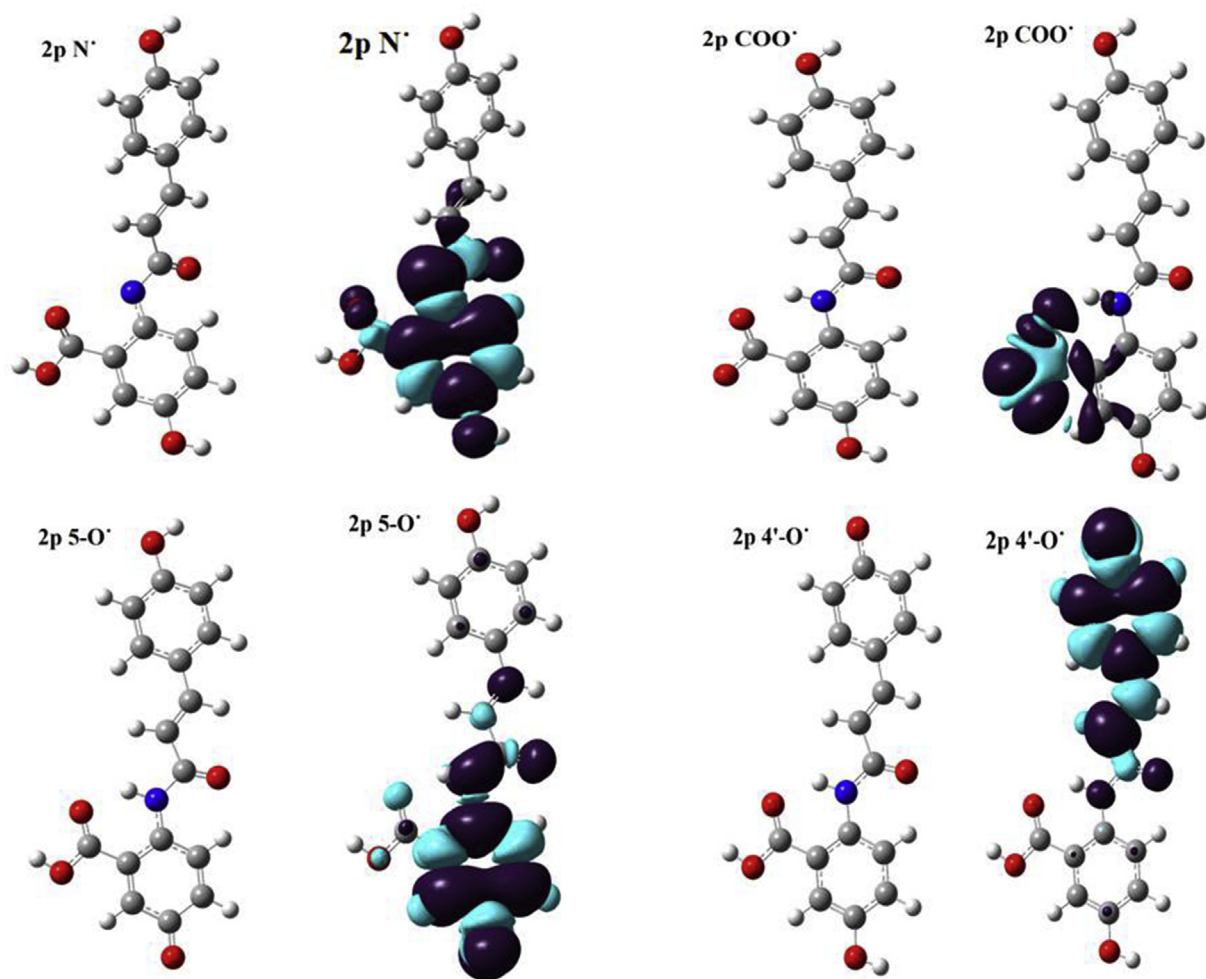


Figure 4. Spin density contour diagrams of 2p showing distribution of electron density when a radical is formed in respective positions.

Table 2. SD values for the O-radical and delocalization index of C–O bond computed for AVs using M062X/6-31G+(d,p) level of theory in the gas phase.

AVs	Parameter	Bond				
		N	COO	5-O	4'-O	3'-O
2p	SD	0.120	0.153	0.087	0.115	-
	DI	1.532	1.898	1.859	1.676	-
2f	SD	0.121	0.153	0.086	0.068	-
	DI	1.532	1.899	1.859	1.913	-
2c	SD	0.120	0.153	0.087	0.071	0.084
	DI	1.532	1.896	1.859	1.872	1.872
1p	SD	0.131	0.153	-	0.076	-
	DI	1.494	1.892	-	1.899	-
1c	SD	0.107	0.153	-	0.071	0.084
	DI	1.512	1.891	-	1.872	1.872
1f	SD	0.138	0.153	-	0.068	-
	DI	1.496	1.894	-	1.914	-
1s	SD	0.139	0.153	-	0.075	-
	DI	1.496	1.892	-	1.880	-
2s	SD	0.120	0.152	0.087	0.075	-
	DI	1.534	1.894	1.859	1.879	-
3f	SD	0.103	0.152	0.085	0.068	-
	DI	1.550	1.881	1.866	1.913	-

4. Conclusion

In this article, the radical scavenging activity of mainly nine avenanthramides (**2p**, **2f**, **2c**, **1p**, **1c**, **1f**, **1s**, **2s**, and **3f**) derived from oats phenolics are computationally explored using DFT-M062X/6-31+G(d, p) level of theory in the gas phase and ethanol. The trans-s-cis conformers of each are found to be the lowest in energy. In the lowest energy structures, compounds **2p**, **2c**, **1p**, **1c**, and **1f** are found to be completely planar and B ring are more aromatic than A-ring. The QTAIM study reveals the existence of hydrogen bonding interaction between NH...C=O of COOH. The IHB between hydroxyl groups of **1c** and **2c** cannot be calculated qualitatively and quantitatively due to the absence of BCP in between them.

Among three mechanisms, the thermodynamically favorable mechanism in the gas phase is HAT whereas SPLET in ethanol. The BDE values are found to be the best correlating with SD and DI values. Also, the trends in BDE are found to be exactly correlating with corresponding experimental shreds of evidence of radical scavenging activity. The hydroxyl group present on the B- ring is more active than the A-ring and the hydroxyl group in the ortho position of the donor hydroxyl group can enhance the activity by stabilizing the radical formed more than the methoxy group. The substitution on B-ring doesn't affect the hydroxyl group of A ring.

Declarations

Author contribution statement

P. C. Sumayya: Conceived and designed the experiments; Analyzed and interpreted the data; Wrote the paper.

Godsa Merin Babu: Performed the experiments; Analyzed and interpreted the data.

K. Muraleedharan: Conceived and designed the experiments; Contributed reagents, materials, analysis tools or data.

Funding statement

This research did not receive any specific grant from funding agencies in the public, commercial, or not-for-profit sectors.

Data availability statement

Data included in article/supplementary material/referenced in article.

Declaration of interests statement

The authors declare no conflict of interest.

Additional information

Supplementary content related to this article has been published online at <https://doi.org/10.1016/j.heliyon.2021.e06125>.

Acknowledgements

The authors express sincere gratitude to the Central Sophisticated Instrumentation Facility (CSIF), University of Calicut for Gaussian 09 software support.

References

- [1] D.M. Peterson, Oat antioxidants, *J. Cereal. Sci.* 33 (2001) 115–129.
- [2] Y. Shi, J. Johnson, M. O'Shea, Y. Chu, The bioavailability and metabolism of phenolics, a class of antioxidants found in grains, *Cereal Foods World* 59 (2014) 52–58.
- [3] L.A. Pham-Huy, H. He, C. Pham-Huy, Free radicals, antioxidants in disease and health, *Int. J. Biomed. Sci.* 4 (2008) 89–96. <https://pubmed.ncbi.nlm.nih.gov/23675073/>.
- [4] V.K. Rajan, C.K. Hasna, K. Muraleedharan, The natural food colorant Peonidin from cranberries as a potential radical scavenger â€ˆ A DFT based mechanistic analysis, *Food Chem.* 262 (2018) 184–190.
- [5] Z. Huyut, Å. Beydemir, Å. Gâ¼dÅ¼in, Antioxidant and antiradical properties of selected flavonoids and phenolic compounds, *Biochem. Res. Int.* 2017 (2017) 7616791.
- [6] Z. Sroka, Antioxidative and antiradical properties of plant phenolics, *Z. Naturforsch. C.* 60 (2005) 833–843.
- [7] L.H. Dimberg, O. Theander, H. Lingnert, Avenanthramides—a group of phenolic antioxidants in oats, *Cereal Chem.* 70 (1993) 637–641. <http://europemc.org/abstr/act/AGR/IND20371739>.
- [8] F.W. Collins, Oat phenolics: avenanthramides, novel substituted N-cinnamoylanthranyl alkaloids from oat groats and hulls, *J. Agric. Food Chem.* 37 (1989) 60–66.
- [9] K. Bratt, K. Sunnerheim, S. Bryngelsson, A. Fagerlund, L. Engman, R.E. Andersson, L.H. Dimberg, Avenanthramides in oats (avena sativa L.) and Structureâ€ Antioxidant activity relationships, *J. Agric. Food Chem.* 51 (2003) 594–600.
- [10] A. Fagerlund, K. Sunnerheim, L.H. Dimberg, Radical-scavenging and antioxidant activity of avenanthramides, *Food Chem.* 113 (2009) 550–556.
- [11] J. Yang, B. Ou, M.L. Wise, Y. Chu, In vitro total antioxidant capacity and anti-inflammatory activity of three common oat-derived avenanthramides, *Food Chem.* 160 (2014) 338–345.
- [12] G. Soycan, M.Y. Schar, A. Kristek, J. Boberska, S.N.S. Alsharif, G. Corona, P.R. Shewry, J.P.E. Spencer, Composition and content of phenolic acids and avenanthramides in commercial oat products: are oats an important polyphenol source for consumers? *T12 - Food Chemistry X* (2020).
- [13] T. Zhang, J. Shao, Y. Gao, C. Chen, D. Yao, Y.F. Chu, J. Johnson, C. Kang, D. Yeo, L.L. Ji, Absorption and elimination of oat avenanthramides in humans after acute consumption of oat cookies, *Oxid. Med. Cell. Longev.* 2017 (2017) 2056705.
- [14] M. Maliarova, T. Maliar, E. KroÅ¼lÅ¼k, J. Sokol, P. NemeÅek, P. NechvÅ¼tal, Antioxidant and proteinase inhibition activity of main oat avenanthramides, *J. Food Nutr. Res.* 54 (2015) 346–353.
- [15] R. Hitayezu, M.M. Baakdah, J. Kinnin, K. Henderson, A. Tsopmo, Antioxidant activity, avenanthramide and phenolic acid contents of oat milling fractions, *J. Cereal. Sci.* 63 (2015) 35–40.
- [16] Y.-F. Chu, M.L. Wise, A.A. Gulvady, T. Chang, D.F. Kendra, B. Jan-Willem van Klinken, Y. Shi, M. O'Shea, In vitro antioxidant capacity and anti-inflammatory activity of seven common oats, *Food Chem.* 139 (2013) 426–431.
- [17] W.J.C. de Bruijn, S. van Dinteren, H. Gruppen, J.-P. Vincken, Mass spectrometric characterisation of avenanthramides and enhancing their production by germination of oat (Avena sativa), *Food Chem.* 277 (2019) 682–690.
- [18] D.J.F.M.J. Frisch, G.W. Trucks, H.B. Schlegel, G.E. Scuseria, M.A. Robb, J.R. Cheeseman, G. Scalmani, V. Barone, G.A. Petersson, H. Nakatsuji, X. Li, M. Caricato, A. Marenich, J. Bloino, B.G. Janesko, R. Gomperts, B. Mennucci, H.P. Hratchian, J.V. Ort, Gaussian 09, Revision A.02, 2016.
- [19] E.E. Bolton, Y. Wang, P.A. Thiessen, S.H. Bryant, in: R.A. Wheeler, D.C.B.T.-A.R., C.C. Spellmeyer (Eds.), Chapter 12 - PubChem: Integrated Platform of Small Molecules and Biological Activities, Elsevier, 2008, pp. 217–241.
- [20] N.M. O'Boyle, M. Banck, C.A. James, C. Morley, T. Vandermeersch, G.R. Hutchison, Open Babel: an open chemical toolbox, *J. Cheminf.* 3 (2011) 33.
- [21] D.G.T.Y. Zhao, N.E. Schultz, Design of density functionals by combining the method of constraint satisfaction with parametrization for thermochemistry, thermochemical kinetics, and noncovalent interactions Title, *J. Chem. Theor. Comput.* 2 (2006) 364–382.
- [22] Y.Z., D.G. Truhlar, The M06 suite of density functionals for main group thermochemistry, thermochemical kinetics, noncovalent interactions, excited states, and transition elements: two new functionals and systematic testing of four M06-class functionals and 12 other function, *Theor. Chem. Acc.* 120 (2008) 215–241.
- [23] T. Lu, F. Chen, Multiwfn: a multifunctional wavefunction analyzer, *J. Comput. Chem.* 33 (2012) 580–592.
- [24] F. Escudero, M. Yâ¼ez, Atoms in molecules, *Mol. Phys.* 45 (1982) 617–628.
- [25] E. Espinosa, E. Molins, C. Lecomte, Hydrogen bond strengths revealed by topological analyses of experimentally observed electron densities, *Chem. Phys. Lett.* 285 (1998) 170–173.
- [26] E.R. Johnson, S. Keinan, P. Mori-Sâ¼nchez, J. Contreras-GarcÃ-a, A.J. Cohen, W. Yang, Revealing noncovalent interactions, *J. Am. Chem. Soc.* 132 (2010) 6498–6506.
- [27] A. MartÃ-nez, M.A. RodrÃ-guez-GironÃ-s, A. Barbosa, M. Costas, Donator acceptor map for carotenoids, melatonin and vitamins, *J. Phys. Chem.* 112 (2008) 9037–9042.
- [28] J.L. Gâ¼zquez, A. Cedillo, A. Vela, Electrodonating and electroaccepting powers, *J. Phys. Chem.* 111 (2007) 1966–1970.
- [29] M. Leopoldini, T. Marino, N. Russo, M. Toscano, Antioxidant properties of phenolic compounds: % H-atom versus electron transfer mechanism, *J. Phys. Chem.* 108 (2004) 4916–4922.
- [30] M. Leopoldini, N. Russo, M. Toscano, The molecular basis of working mechanism of natural polyphenolic antioxidants, *Food Chem.* 125 (2011) 288–306.
- [31] G. Litwinienko, K.U. Ingold, Solvent effects on the rates and mechanisms of reaction of phenols with free radicals, *Acc. Chem. Res.* 40 (2007) 222–230.
- [32] G. Litwinienko, K.U. Ingold, Abnormal solvent effects on hydrogen atom abstraction. 2. Resolution of the curcumin antioxidant controversy. The role of sequential proton loss electron transfer, *J. Org. Chem.* 69 (2004) 5888–5896.

- [33] M. Musialik, G. Litwinienko, Scavenging of dpph• radicals by vitamin E is accelerated by its partial ionization: the role of sequential proton loss electron transfer, *Org. Lett.* 7 (2005) 4951–4954.
- [34] I. Nakanishi, T. Kawashima, K. Ohkubo, H. Kanazawa, K. Inami, M. Mochizuki, K. Fukuhara, H. Okuda, T. Ozawa, S. Itoh, S. Fukuzumi, N. Ikota, Electron-transfer mechanism in radical-scavenging reactions by a vitamin E model in a protic medium, *Org. Biomol. Chem.* 3 (2005) 626–629.
- [35] D. Kozłowski, P. Trouillas, C. Calliste, P. Marsal, R. Lazzaroni, J.-L. Duroux, Density functional theory study of the conformational, electronic, and antioxidant properties of natural chalcones, *J. Phys. Chem.* 111 (2007) 1138–1145.
- [36] J.R. Lane, J. Contreras-García, J.-P. Piquemal, B.J. Miller, H.G. Kjaergaard, Are bond critical points really critical for hydrogen bonding? *J. Chem. Theor. Comput.* 9 (2013) 3263–3266.
- [37] J. Poater, X. Fradera, M. Duran, M. Solà, The delocalization index as an electronic aromaticity criterion: application to a series of planar polycyclic aromatic hydrocarbons, *Chem. Eur J.* 9 (2003) 400–406.
- [38] E. Matito, M. Duran, M. Solà, The aromatic fluctuation index (FLU): a new aromaticity index based on electron delocalization, *J. Chem. Phys.* 122 (2004) 14109.
- [39] G.M. Bruno, C.G., Leonardo Lo Presti, Spin density topology, *Molecules* 25 (2020) 3537.
- [40] E. Matito, J. Poater, M. Solà, M. Duran, P. Salvador, Comparison of the AIM delocalization index and the mayer and fuzzy atom bond orders, *J. Phys. Chem.* 109 (2005) 9904–9910.
- [41] T.K. Shameera Ahamed, V.K. Rajan, K. Sabira, K. Muraleedharan, DFT and QTAIM based investigation on the structure and antioxidant behavior of lichen substances Atranorin, Evernic acid and Diffracta acid, *Comput. Biol. Chem.* 80 (2019) 66–78.